Synthesis and Thermal Cure of Anthracenyl−Ethynyl End-Capped Imide Oligomers

Michael E. Wright* and Derek A. Schorzman

Department of Chemistry, Virginia Commonwealth University, Richmond, Virginia 23284-2006

Received February 26, 2001; Revised Manuscript Received April 23, 2001

ABSTRACT: The model compound, *N*-phenyl-4-(9-anthracenylethynyl)phthalimide (**3**), was synthesized and the thermal curing behavior analyzed. These results were compared to the curing kinetics of similar model compounds *N*-phenyl-4-(1-naphthylethynyl)phthalimide (**1**) and *N*-phenyl-4-phenylethynylphthalimide (**2**). The cure rates are found to increase in the order of phenyl < naphthyl ≪ anthracenyl with indistinguishable E_a values for **1** and **2**. Compound **3** showed a slightly lower E_a for the curing process. The end-capping reagent 4-(9-anthracenylethynyl)phthalic anhydride (4-AnEPA, **4**) was prepared and used to synthesize an "anthracenyl−ethynyl terminated imide oligomer" (AnETI-**5**) and a lower T_g anthracenyl−ethynyl terminated imide-*co*-oxydiphthalic anhydride oligomer (AnETI-**5**-ODPA). Kinetic data for the thermal cure of the oligomers were measured by monitoring the change in T_g and applying the DiBenedetto equation. To ensure consistency, the thermal cure kinetics of phenyl−ethynyl terminated imide oligomer (PETI-**5**), naphthyl−ethynyl terminated imide oligomer (NETI-**5**), and phenyl−ethynyl terminated imide-*co*-oxydiphthalic anhydride oligomer (PETI-**5**-ODPA) were co-analyzed. The T_g observed for the cured resins was found to be independent of the end-cap type. However, the new aryl−ethynyl end caps provide significant thermal cure rate acceleration, often without a change in the E_a. For example, the anthracenyl−ethynyl end-capped oligomers can be cured at the same rate as the phenyl−ethynyl analogue; however, at a temperature nearly 80 °C lower!

Introduction

Phenyl−ethynyl terminated imide oligomers can be thermally cured to afford resins with excellent chemical and mechanical properties for use in high-performance applications.[1−16] Neat thermal curing is performed at temperatures above the T_g of the oligomer, typically 370 °C for 1 h. The cured phenyl−ethynyl terminated resins possess improved thermo-oxidative stability and processability over thermally cured acetylene terminated imide oligomer resins.[17−20] Various cross-linking/chain-extension reactions of the acetylene moiety have been suggested,[4,5,8] but the structure of and the reaction(s) leading to the final resin remain uncertain. Although the reaction(s) leading to the cured resin appear to be multifaceted,[8,12] recent thermal cure kinetic analyses reveal pseudo-first-order rate laws for several phenyl−ethynyl end-capped model compounds.[1,2,6,8] Several of the analogous doubly end-capped oligomers have also demonstrated pseudo-first-order curing rates for at least a majority of the curing process and are in good agreement with the model compounds.[1,3,6,8]

Substituents both on the terminal phenyl[14] and replacing the imide functionality[3] have been shown to modify the thermal curing rates for model compounds and oligomer structures. How substituent effects are influencing the reaction pathway remains unclear and deserves continued attention from researchers in the field.

Recently, we have reported on a new modification of the end cap that effectively lowers the curing temperature necessary for an equivalent cure rate.[1,6] Replacement of the terminal phenyl−ethynyl with a 1-naphthyl−ethynyl group resulted in equivalent cure rates at approximately a 30 °C lower cure temperature. Importantly, this result was accompanied by no significant change in the many desirable properties of the phenyl−ethynyl end-capped oligomers and of the thermally cured resins. In the present study, we demonstrate that this trend in rate acceleration can be taken further by substituting anthracenyl−ethynyl as the end cap on the imide oligomers. Herein we report on the synthesis and kinetic analyses of this new aryl−ethynyl end cap both at the model level and on two different imide oligomers.

Results and Discussion

Model Compounds and Imide Oligomer Synthesis. The model compound *N*-phenyl-4-(9-anthracenylethynyl)phthalimide (**3**) and the end-capping reagent 4-(9-anthracenylethynyl)phthalic anhydride (4-AnEPA) were synthesized using standard ethynylation techniques.[21] Model compounds **1**[8,13] and **2**[1,6] have been previously synthesized and analyzed.

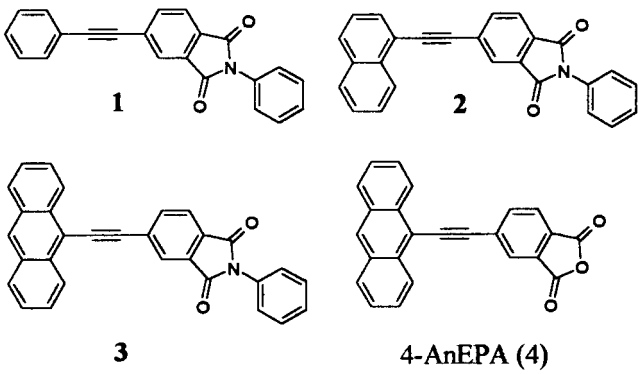

Anthracenyl−ethynyl terminated imide oligomer (AnETI-**5**), phenyl−ethynyl terminated imide-*co*-oxydiphthalic anhydride oligomer (PETI-**5**-ODPA), and anthracenyl−ethynyl terminated imide-*co*-oxydiphthalic anhydride oligomer (AnETI-**5**-ODPA), were synthesized using a slight modification of the previously reported technique to a theoretical M_n of 5000 g/mol (Table 1).[11]

10.1021/ma010339l CCC: $20.00
Published on Web 06/09/2001

Table 1. Analysis of Oligomers Using DSC and SEC

	sample				
	PETI-**5**	NETI-**5**	AnETI-**5**	PETI-**5**-ODPA	AnETI-**5**-ODPA
M_w	3400	2900	2700	4500	5000
PD	1.8	1.7	1.3	1.7	1.5
T_m (°C)	263	264	218	177	209
T_{gu} (°C)	237	230	222	190	199
T_{gc} (°C)	265	263	259	234	235

The structure of AnETI-**5** differs from PETI-**5** only by the substitution of the 9-anthracenyl−ethynyl for the phenyl−ethynyl end cap. Synthesis of the phenyl−ethynyl terminated imide oligomer (PETI-**5**)[11] and naphthyl−ethynyl terminated imide oligomer (NETI-**5**)[1] were previously reported using the same technique. AnETI-**5**-ODPA was synthesized to incorporate additional ether linkages in conjunction with the 4-AnEPA end cap and the analogous phenyl−ethynyl end-capped PETI-**5**-ODPA was synthesized for comparison purposes. Structures are shown in Chart 1.

Model Curing Reactions. Curing of the model compound and oligomers was carried out by placing samples in Pyrex reaction vessels which were then purged with nitrogen, evacuated, and then sealed by torch. Each sample in a particular kinetic run was placed in a calibrated and temperature stabilized aluminum heating block and removed at the proper time interval. The sample vessel was opened and the material dissolved in the appropriate solvent and analyzed by either NMR spectroscopy or chromatography.

In the case of **3** inadequate solubility in standard deuterated solvents (e.g., $CDCl_3$, d_6-acetone, d_6-DMSO) made data collection by ^{1}H NMR spectroscopy difficult and led to significant data inconsistencies. However, complete solubility of **3** at the low concentrations required for SEC analysis made this a suitable technique. From our previous studies comparing **1** and **2**, we found excellent agreement using the two different experimental techniques of ^{1}H NMR and SEC.[1,6] Hence, samples of **3** at different curing times were dissolved in THF (∼2 mg/mL) and then injected onto a SEC column for analysis. The molecular weights are reported relative to polystyrene standards. The SEC traces of **3** are very similar to those measured in the case of **1** and **2** (Figure 1). In all three cases, approximately a dimeric/trimeric structure appears to be formed with no indication of higher molecular weight product being observed, even as the reaction approaches completion. Extent of reaction was determined by integration of the reactant peak relative to the normalized trace. Analysis of the data using first-order rate laws (i.e., $\ln(C/C_0)$ vs time) provides a good line fit and the needed rate constants. An Arrhenius plot (Figure 2) was used to determine the energy of activation (E_a), and an Eyring plot (i.e. $\ln[(C/C_0)/T]$ vs $1/T$) was employed to determine transition-state parameters (see Tables 2 and 3). For comparison purposes, kinetic analyses of **1** and **2** using SEC were also performed and compared to ^{1}H NMR data previously collected in our laboratory (see Table 4).[1]

Imide Oligomer Curing Reactions. The thermal cure kinetics of the oligomeric systems PETI-**5**, NETI-**5**, AnETI-**5**, PETI-**5**-ODPA, and AnETI-**5**-ODPA were determined by monitoring the change in glass transition temperature (T_g) using DSC. Cured samples were removed from the heating block and then analyzed on a Perkin-Elmer DSC-7 (under nitrogen, flow rate of 40 cm^3/min, ramp rate of 10 °C/min). The extent of cure was calculated using the DiBenedetto equation,[22−25] modified for highly cross-linked networks

$$(T_g - T_{gu})/(T_{gc} - T_{gu}) = \lambda x/(1 - (1 - \lambda)x)$$

where T_g represents the glass transition temperature of the model compound after thermal curing at each temperature, T_{gu} is the glass transition temperature of the uncured model compound, T_{gc} is the glass transition temperature of fully cured model compound, λ is the ratio of the isobaric heat capacity of fully cured model compound to that of uncured model compound, and x is the reaction extent (i.e. $C/C_0 = 1 - x$).

Analysis of uncured oligomers using DSC (Figure 3) revealed a single peak (T_m) in the first scan and a well-defined T_g in the second scan (T_{gu}) of the uncured material and in the fully cured sample (380 °C for 1 h, T_{gc}). These values of T_{gu} and T_{gc} were used in our calculations (Table 1) and the λ value determined by Scola and co-workers[8] for PETI-**5** was used in our calculations ($\lambda = 0.69$) for all oligomers. As previously noted, structural changes in the end cap have little or no effect on the properties of the oligomers.[1] The different end caps change the T_m, T_{gu}, and T_{gc} values; however, these small changes might be due in part to the differences in oligomeric chain length and some due to errors in measuring these experimental values. Supporting this idea is that the differences in T_{gc} prove to be quite small.[1] By applying first-order data analysis, we obtained uniformly good line fits and used the observed rate constants in Arrhenius and Eyring plots (see Figures 4 and 5, respectively).

Discussion of the Curing Reactions/Kinetics. Arrhenius (Figure 2, Table 2) and Eyring (Table 3) analyses of the thermal curing of **1** and **2** reveal a good correlation between the two methods of SEC and ^{1}H NMR analysis. Because of an overlap between the cured and uncured peaks in the SEC traces, some deviation from the ^{1}H NMR data occurs at the beginning of each kinetic run. This is especially apparent for the case of **1** at low temperatures since the curing process is very slow. Since the E_a values for **1** and **2** are statistically indistinguishable, the observed rate acceleration must be attributed to differing preexponential factors (A). Model compound **3** cures at a much faster rate and with a slightly lower E_a than **1** and **2**. Thus, **3** can be cured at the same rate as **1** at approximately a 55 °C lower temperature (Table 4). This rate acceleration trend (phenyl < naphthyl ≪ anthracenyl) is in contrast with the increasing steric bulk about the acetylene bond; however, it does nicely correlate with a trend in the calculated first-order polarizability.[26]

Kinetic analysis of the thermal cure of the analogous oligomers using DSC reveals the same rate acceleration trend of phenyl < naphthyl ≪ anthracenyl (Figure 4). At the temperatures studied so far, the rate acceleration for AnETI-**5** over PETI-**5** permits the former to be cured at approximately a 80 °C lower temperature. What remains fascinating is the fact that the increase in cure rate is done with little or no change in the E_a for AnETI-**5**.

The phenyl−ethynyl and anthracenyl−ethynyl end-capped oligomers incorporating additional ether linkages also exhibit significantly different curing rates with statistically indistinguishable E_a values (Figure 5). Our results show that the *aryl*ETI-**5**-ODPA oligomers cure faster in comparison to their repective *aryl*ETI-**5** counterparts. Interestingly, we find that in the lower T_g material AnETI-**5**-ODPA the temperature difference (for

Chart 1. Aryl−Ethynyl Terminated Imide Oligomers

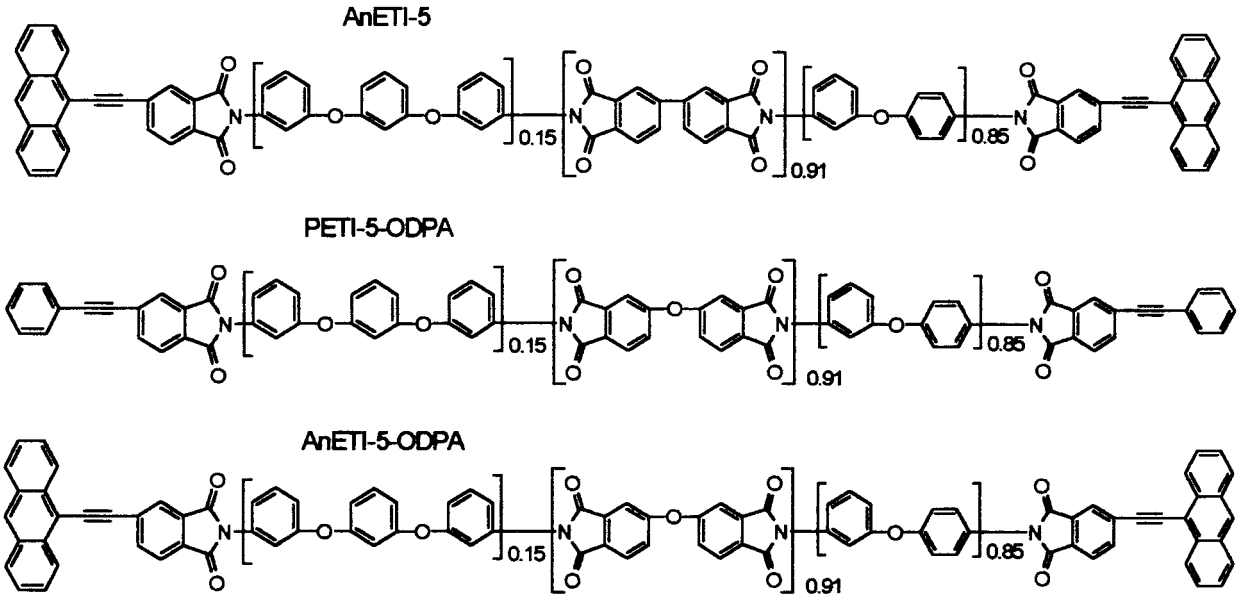

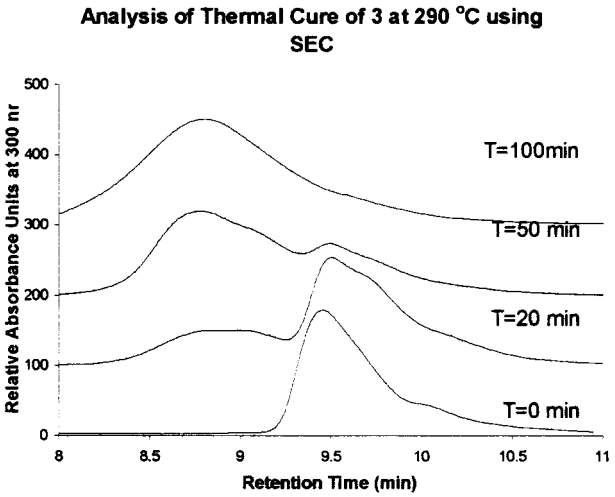

Figure 1. Traces of SEC monitoring the progress of curing for model compound **3** at 290 °C.

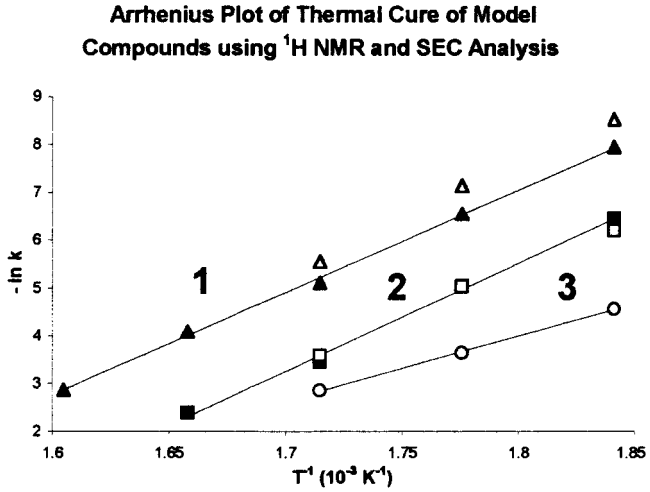

Figure 2. Arrhenius plot of thermal cure of model compounds **1** (▲), **2** (■), and **3** (○). For analysis ^{1}H NMR spectroscopy solid symbols are displayed and for SEC data hollow symbols are used. DSC analysis for the curing of imide oligomer AnETI-**5**.

a comparable cure rate) is ∼55 °C in comparison to ∼80 °C for the higher T_g oligomeric materials.

Concluding Remarks

The present study demonstrates a method in which to modify the kinetics of the thermal curing of phenyl−ethynyl end-capped oligomers by simple substitution of the terminal aromatic ring, resulting in rate accelerations of up to 80 °C, depending on the oligomer backbone. We find once again that kinetic data measured for model compounds correlates well to that found for the curing of oligomeric structures. The rate acceleration due to the anthracenyl−ethynyl end cap is the largest in each of the three systems presented. In terms of steric considerations this is somewhat counterintuitive. The measured rate acceleration must be dominated by differences in the preexponential constant (A) and not lower E_a values. This strongly suggests that a difference in stereoelectronics, collisional factors, and other parameters accounted for in A are the major factor(s) in the rate enhancement. On the other hand, at this point in time, we cannot rule out a change in mechanism for the anthracenyl−ethynyl system.

It is also quite interesting to note that the calculated dipole moments for **1**, **2**, and **3** are nearly identical. In contrast, their calculated first order polarizability increases significantly from **1** to **3**.[26] We are currently pursuing calculation methods coupled with the synthesis and kinetic analysis of substituted naphthyl− and anthracenyl−ethynyl model compounds to gain further insight in the curing mechanism. In addition, we are beginning to study these controlled and highly active curing agents on a variety of polymer backbones and functionality.

Experimental Section

General Methods. All manipulations of compounds and solvents were carried out using standard Schlenk techniques. Tetrahydrofuran (THF) and triethylamine were purified by distillation under nitrogen from standard drying agents. *N*-Methylpyrrolidinone was dried over molecular sieves prior to use. ^{1}H and ^{13}C NMR measurements were performed using a Varian Oxford 300 MHz instrument. NMR chemical shifts are reported vs Me_4Si in ^{1}H NMR spectra and by assigning the $CDCl_3$ resonance at 76.90 ppm in ^{13}C NMR spectra. The

Table 2. Experimental Arrhenius Parameters of All Model Compounds and Oligomers[a]

	2	**1**	**2**	**1**	**3**	PETI-**5**	NETI-**5**	AnETI-**5**	PETI-**5**-ODPA	AnETI-**5**-ODPA
method	^{1}H NMR[1,6]	^{1}H NMR[1,6]	SEC	SEC	SEC	DSC	DSC	DSC	DSC	DSC
R^2	0.9969	0.9986	0.9967	0.9966	0.9994	0.9830	0.9992	0.9832	0.9759	0.9906
slope	−22639 (897)	−21411 (464)	−20652 (1692)	−23565 (1385)	−13584 (320)	−18650 (2456)	−19879 (568)	−15880 (1468)	−15789 (1753)	−17075 (1173)
intercept	35.2 (16)	31.5 (8)	31.8 (30)	34.8 (25)	20.5 (6)	25.3 (40)	28.3 (9)	24.7 (25)	22.3 (31)	27.0 (21)
E_a (kJ/mol)	188 (8)	178 (4)	172 (14)	196 (12)	113 (3)	155 (20)	165 (5)	132 (12)	131 (15)	142 (10)
A (min^{-1})	2×10^{15}	5×10^{13}	6×10^{13}	1×10^{15}	8×10^{8}	1×10^{11}	2×10^{12}	5×10^{10}	5×10^{9}	5×10^{11}

[a] Number in parentheses represents standard deviation error for the last significant digit(s).

Table 3. Experimental Eyring Parameters of All Model Compounds and Oligomers[a]

	2	**1**	**2**	**1**	**3**	PETI-**5**	NETI-**5**	AnETI-**5**	PETI-**5**-ODPA	AnETI-**5**-ODPA
method	^{1}H NMR[1,6]	^{1}H NMR[1,6]	SEC	SEC	SEC	DSC	DSC	DSC	DSC	DSC
R^2	0.9967	0.9985	0.9965	0.9964	0.9994	0.9819	0.9991	0.9818	0.9740	0.9900
slope	−22067 (899)	−20830 (466)	−20089 (1686)	−23003 (1379)	−13021 (326)	−18027 (2450)	−19256 (573)	−15308 (1474)	−15217 (1757)	−16523 (1174)
intercept	27.9 (16)	24.1 (8)	24.4 (30)	27.5 (25)	13.1 (6)	17.9 (39)	20.9 (9)	17.4 (26)	14.9 (31)	19.7 (21)
ΔH_{act} (kJ/mol)	183 (8)	173 (4)	167 (14)	191 (12)	108 (3)	150 (20)	160 (5)	127 (12)	127 (15)	137 (10)
ΔS_{act} (J/(K mol))	34 (13)	3 (7)	5 (25)	31 (20)	−89 (5)	−49 (33)	−24 (8)	−54 (21)	−74 (26)	−35 (18)

[a] Number in parentheses represent standard deviation error for the last significant digits.

Table 4. Experimental Rate Values for All Model Compounds and Oligomers at All Temperatures

analysis	sample	250 °C	270 °C	290 °C	310 °C	330 °C	350 °C	370 °C
^{1}H NMR[1,6]	**2**		1.57×10^{-3}	6.53×10^{-3}	3.18×10^{-2}	9.26×10^{-2}		
^{1}H NMR[1,6]	**1**		3.53×10^{-4}	1.43×10^{-3}	6.09×10^{-3}	1.68×10^{-2}	5.71×10^{-2}	
SEC	**2**		2.04×10^{-3}	6.55×10^{-3}	2.78×10^{-2}			
SEC	**1**		1.98×10^{-4}	7.97×10^{-4}	3.90×10^{-3}			
SEC	**3**		1.04×10^{-2}	2.62×10^{-2}	5.79×10^{-2}			
DSC	NETI-**5**					9.56×10^{-3}	2.90×10^{-2}	7.42×10^{-2}
DSC	PETI-**5**					3.95×10^{-3}	8.58×10^{-3}	2.72×10^{-2}
DSC	AnETI-**5**		9.27×10^{-3}	3.57×10^{-2}	8.89×10^{-2}	1.71×10^{-1}		
DSC	PETI-**5**-ODPA		1.06×10^{-3}	2.97×10^{-3}	1.09×10^{-2}	1.69×10^{-2}		
DSC	AnETI-**5**-ODPA	3.57×10^{-3}	9.88×10^{-3}	4.17×10^{-2}	9.20×10^{-2}			

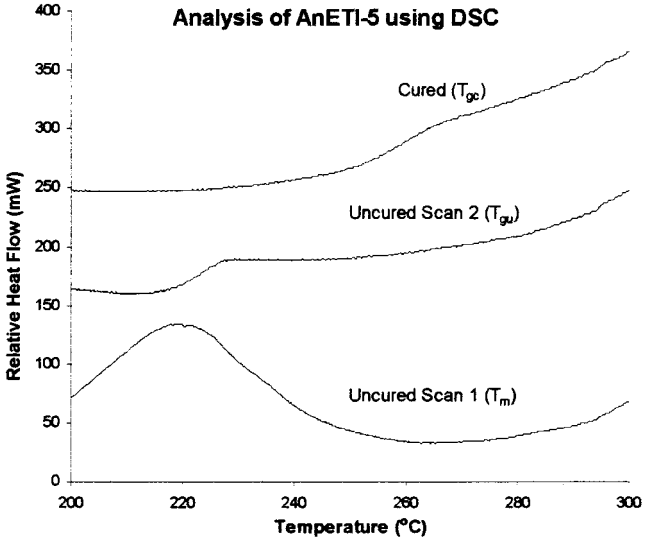

Figure 3. DSC scans of AnETI-**5** oligomer and cured resin. DSC scans were run under a nitrogen atmosphere and at a ramp rate of 10 °C/min.

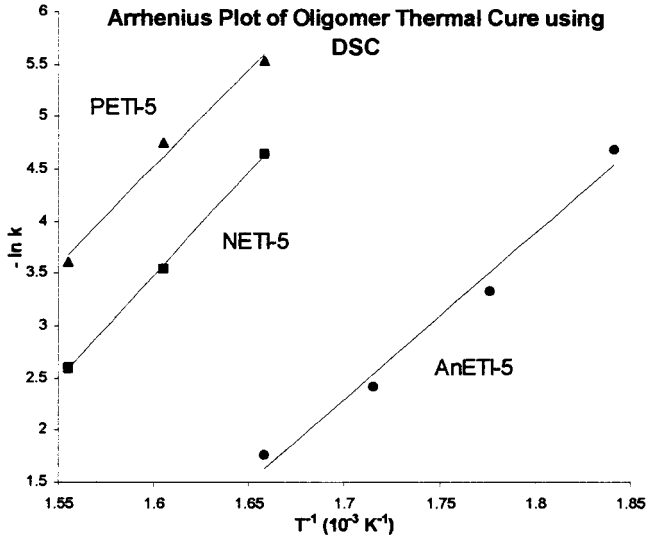

Figure 4. Arrhenius plot for the thermal cure of PETI-**5** (▲), NETI-**5** (■), and AnETI-**5** (●) using kinetic data by DSC analysis.

compounds 9-bromoanthracene, 3,4′-oxydianiline, and 3,3′,4,4′-biphenyltetracarboxylic anhydride were purchased from Aldrich Chemical Co. The compounds 1,3-bis(3-aminophenoxy)-benzene and 4,4′-oxydiphthalic anhydride were purchased from TCI America and trimethylsilylacetylene was purchased from GFS Chemicals, Inc. 4-Bromophthalic anhydride was supplied by NASA, Langley, VA. SEC analyses were performed by dilution in THF (2 mg/mL) and then injection onto a Hewlett-Packard 1100 HPLC (column: PL 300 × 7.5 mm, 5 μm particle size). Molecular weights are calculated relative to polystyrene standards. Elemental analyses were performed at Atlantic Microlab Inc., Norcross, GA.

Synthesis of *N*-Phenyl-4-(9-anthracenylethynyl)phthalimide (3). To a solution of 9-bromoanthracene (5.14 g, 20.0 mmol), triphenylphosphine (525 mg, 2.0 mmol), cuprous iodide (190 mg, 1.0 mmol), and bis(triphenylphosphine)palladium dichloride (280 mg, 0.40 mmol) in 1:1 benzene/triethylamine (60 mL) was added trimethylsilylacetylene (2.95 g, 30.0 mmol). The solution was stirred at room temperature (30 min) and heated at reflux (90 min). The cooled solution was diluted with ether (200 mL) and vacuum filtered. The filtrate was washed with H_2O (3 × 150 mL) and brine (1 × 100 mL) and dried over Na_2SO_4. The solvents were removed under reduced pressure to yield crude 9-(trimethylsilylethynyl)anthracene

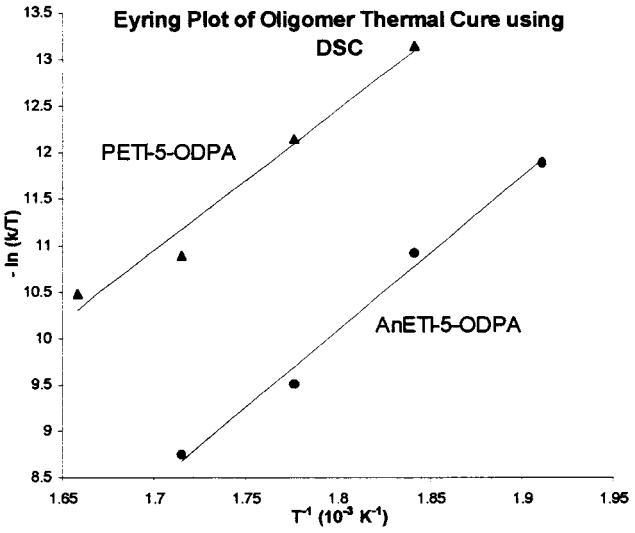

Figure 5. Arrhenius plot for thermal cure kinetic data of PETI-**5**-ODPA (▲) and AnETI-**5**-ODPA (●) obtained from DSC analysis.

(6.95 g). The crude 9-(trimethylsilylethynyl)anthracene was dissolved in methanol (200 mL) and 3.5 M KOH(aq) (2 mL) was added. The solution was stirred 1 h and quenched with H_2O (200 mL). The mixture was extracted with hexane (200 mL), and the organic was washed with H_2O (3 × 150 mL) and brine (1 × 100 mL) and dried over Na_2SO_4. The solvents were removed under reduced pressure to yield crude 9-anthracenylacetylene (3.45 g, 17.1 mmol). The crude 9-anthracenylacetylene was dissolved in benzene (65 mL) and added by cannula transfer to a solution of *N*-phenyl-4-bromophthalimide (3.59 g, 11.9 mmol), triphenylphosphine (310 mg, 1.2 mmol), cuprous iodide (110 mg, 0.6 mmol), and bis(triphenylphosphine)palladium dichloride (170 mg, 0.2 mmol) in 2:1 triethylamine/benzene (200 mL) and heated at reflux for 3 h. The mixture was cooled to 0 °C and filtered. The filtrate was added to H_2O (300 mL), stirred vigorously for 1 h, and filtered. The filtrate was washed with H_2O (3 × 10 mL) and dried to constant weight under reduced pressure at 85 °C. The crude product was hot filtered and recrystallized from toluene to yield *N*-phenyl-4-(9-anthracenylethynyl)phthalimide (3.15 g, 37.2%) as an orange solid (mp 238−40 °C). λ_{max} = 442 nm. ^{1}H NMR ($CDCl_3$, 300 MHz): δ 7.43−7.58 (m, 6H), 7.64−7.69 (m, 3H), 8.01−8.07 (m, 3H), 8.14 (d, J = 7.7 Hz, 1H), 8.31 (s, 1H), 8.52 (s, 1H), 8.62 (d, J = 8.6 Hz, 2H). ^{13}C NMR ($CDCl_3$, 300 MHz): δ 91.7, 99.2, 115.9, 124.1, 126.1, 126.5, 126.6, 126.7, 127.5, 128.4, 129.1, 129.4, 130.5, 131.3, 131.8, 132.3, 133.1, 137.2, 166.8, 166.9. Anal. Calcd for $C_{30}H_{17}NO_2$: C, 85.09; H, 4.05. Found: C, 84.86; H, 4.04.

Synthesis of 4-(9-Anthracenylethynyl)phthalic Anhydride (4). To a solution of 9-bromoanthracene (1.35 g, 5.25 mmol), triphenylphosphine (138 mg, 0.53 mmol), copper iodide (50 mg, 0.26 mmol), and bis(triphenylphosphine)palladium dichloride (74 mg, 0.11 mmol) in 1:1 triethylamine/benzene (35 mL) was added trimethylsilylacetylene (1.11 mL, 7.85 mmol), and the solution was heated at reflux 1 h. The cooled solution was diluted with ethyl ether (100 mL) and filtered. The organic was washed with H_2O (3 × 100 mL), dried over Na_2SO_4, and filtered. Solvents were removed under reduced pressure to yield crude 9-anthracenyltrimethylsilylacetylene. The crude oil was dissolved in methanol (150 mL) and 3.5 M KOH(aq) (2 mL) was added and stirred for 1 h. The reaction was quenched with H_2O (150 mL), and the product was extracted with hexane (3 × 100 mL). The combined organic layers were dried over Na_2SO_4 and filtered, and solvents were removed under reduced pressure to yield crude 9-anthracenylacetylene. The crude oil was dissolved in benzene (10 mL) and added to a solution of 4-bromophthalic anhydride (0.908 g, 4.0 mmol), triphenylphosphine (105 mg, 0.40 mmol), copper iodide (39 mg, 0.20 mmol), and bis(triphenylphosphine)-palladium dichloride (56 mg, 0.08 mmol) in 2:1 triethylamine/benzene (30 mL) by cannula transfer and heated at reflux 1 h. The cooled solution was filtered and the precipitate was diluted with 0.5 M $NaHCO_3$(aq) (100 mL) and stirred vigorously for 1 h. The mixture was diluted with acetone (50 mL) and filtered. The crude product was recrystallized from toluene and dried under reduced pressure to yield 4-(9-anthracenylethynyl)phthalic anhydride (1.03 g, 73.8%) as a deep red solid (mp 254−257 °C). ^{1}H NMR (DMSO-d_6, 300 MHz): δ 7.77 (t, J = 7.1 Hz, 2H), 7.88 (t, J = 7.2 Hz, 2H), 8.29−8.34 (m, 3H), 8.56 (d, 7.8 Hz, 1H), 8.75 (s, 1H), 8.83 (d, J = 8.7 Hz, 2H), 8.92 (s, 1H). ^{13}C NMR (DMSO-d_6, 300 MHz): δ 91.1, 98.8, 114.5, 125.6, 126.0, 126.1, 126.2, 127.7, 127.8, 127.9, 129.0, 129.7, 130.6, 132.3, 138.5, 162.69. Anal. Calcd for $C_{24}H_{12}O_3$: C, 82.75; H, 3.47. Found: C, 82.16; H, 3.51.

Synthesis of Anthracenyl−Ethynyl Terminated Imide oligomer (AnETI-5). To a solution of 1,3-bis(3-aminophenoxy)benzene (0.15 equiv, 0.19 g, 0.66 mmol) and 3,4′-oxydianiline (0.85 equiv, 0.75 g, 3.8 mmol) in *N*-methylpyrrolidinone (35 mL) were added 3,3′,4,4′-biphenyltetracarboxylic dianhydride (0.91 equiv, 1.18 g, 4.02 mmol) and 4-(9-anthracenylethynyl)phthalic anhydride (0.18 equiv, 0.28 g, 0.79 mmol). The solution was stirred under nitrogen at ambient temperature for 20 h. The flask was equipped with a Dean−Stark trap and condenser, toluene was added (100 mL), and the mixture was heated at reflux for 20 h. The cooled solution was added to water (150 mL) and the precipitate was filtered and washed successively with warm water (3 × 10 mL) and methanol (3 × 10 mL). The powders were then dried at 85 °C and reduced pressure to constant weight to yield light orange AnETI-**5** (1.88 g, 84.3%): M_n = 2736; PD = 1.29.

Synthesis of Phenyl−Ethynyl Terminated Imide-*co*-Oxydiphthalic Anhydride Oligomer (PETI-5-ODPA). To a solution of 1,3-bis(3-aminophenoxy)benzene (0.15 equiv, 0.19 g, 0.66 mmol) and 3,4′-oxydianiline (0.85 equiv, 0.75 g, 3.8 mmol) in *N*-methylpyrrolidinone (35 mL) were added 4,4′-oxydiphthalic anhydride (0.91 equiv, 1.25 g, 4.02 mmol) and 4-phenylethynylphthalic anhydride (0.18 equiv, 0.20 g, 0.79 mmol). The solution was stirred under nitrogen at ambient temperature for 20 h. The flask was equipped with a Dean−Stark trap and condenser, toluene was added (100 mL), and the mixture was heated at reflux for 20 h. The cooled solution was added to water (150 mL), and the precipitate was filtered and washed successively with warm water (3 × 10 mL) and methanol (3 × 10 mL). The powders were then dried at 85 °C and reduced pressure to constant weight to yield colorless PETI-**5**-ODPA (1.94 g, 81.3%): M_n = 4485; PD = 1.72.

Synthesis of Anthracenyl−Ethynyl Terminated Imide-*co*-Oxydiphthalic Anhydride Oligomer (AnETI-5-ODPA). To a solution of 1,3-bis(3-aminophenoxy)benzene (0.15 equiv, 0.19 g, 0.66 mmol) and 3,4′-oxydianiline (0.85 equiv, 0.75 g, 3.8 mmol) in *N*-methylpyrrolidinone (35 mL) were added 4,4′-oxydiphthalic anhydride (0.91 equiv, 1.25 g, 4.02 mmol) and 4-(9-anthracenylethynyl)phthalic anhydride (0.18 equiv, 0.28 g, 0.79 mmol). The solution was stirred under nitrogen at ambient temperature for 20 h. The flask was equipped with a Dean−Stark trap and condenser, toluene was added (100 mL), and the mixture was heated at reflux for 20 h. The cooled solution was added to water (150 mL) and the precipitate was filtered and washed successively with warm water (3 × 10 mL) and methanol (3 × 10 mL). The powders were then dried at 85 °C and reduced pressure to constant weight to yield light yellow AnETI-**5**-ODPA (1.55 g, 64.4%): M_n = 5033; PD = 1.52.

DSC Analysis of the Curing Reaction. Kinetic samples were pulled from the curing chamber and then loaded into aluminum DSC pans (~10 mg sample size). The DSC samples were covered (not sealed) and then placed in the Perkin-Elmer DSC-7 instrument. The sample chamber was purged with nitrogen (40 cm^3/min) and the data collected with a ramp rate of 10 °C/min. The T_g was calculated using the DSC-7 software and then confirmed by hand.

Acknowledgment. The authors wish to thank the Office of Naval Research for partial funding of this work.

References and Notes

(1) Wright, M. E.; Schorzman, D. A.; Pence, L. E. *Macromolecules* **2000**, *33*, 8611−8617.
(2) Holland, T. V.; Glass, T. E.; McGrath, J. E. *Polymer* **2000**, *41*, 4965−4990.
(3) Ayambem, S. J.; Mecham, S. J.; Sun, Y.; Glass, T. E.; McGrath, J. E. *Polymer* **2000**, *41*, 5109−5124.
(4) Cho, D.; Drzal, L. T. *J. Appl. Polym. Sci.* **2000**, *76*, 190−200.
(5) Fang, X.; Xie, X.-Q.; Simone, C. D.; Stevens, M. P.; Scola, D. A. *Macromolecules* **2000**, *33*, 1671.
(6) Wright, M. E.; Schorzman, D. A. *Macromolecules* **1999**, *32*, 8693−8694.
(7) Preston, C. M. L.; Jill, D. J. T.; Pomery, P. J.; Whittaker, A. K.; Jensen, B. J. *High Perform. Polym.* **1999**, *11*, 453−465.
(8) Fang, X.; Rogers, D. F.; Scola, D. A.; Stevens, M. P. *J. Polym. Sci.* **1998**, *36*, 461−470.
(9) Connell, J. W.; Smith, J. G., Jr.; Hergenrother, P. M. *High Perform. Polym.* **1998**, *10*, 273−283.
(10) Jayaraman, S.; Srinivasan, R.; McGrath, J. E. *J. Polym. Sci., Part A* **1995**, *33*, 1551−1563.
(11) Hergenrother, P. M.; Smith, J. G., Jr. *Polymer* **1994**, *35*, 4857.
(12) Hinkley, J. A. *J. Adv. Mater.* **1994**, *27*, 55−59.
(13) Takekoshi, T.; Terry, J. M. *Polymer* **1994**, *35*, 4874−4880.
(14) Johnston, J. A.; Li, F. M.; Harris, F. W.; Takekoshi, T. *Polymer* **1994**, *35*, 4865−4873.
(15) Jensen, B. J.; Hergenrother, P. M. *J. Macromol. Sci.—Pure Appl. Chem.* **1993**, *A30* (6&7), 449−458.
(16) Douglas, W. E.; Overend, A. S. *Eur. Polym. J.* **1993**, *29*, 1513.
(17) Sastri, S. B.; Keller, T. M.; Jones, K. M.; Armistead, J. P. *Macromolecules* **1993**, *26*, 6171−6174.
(18) Swanson, S. A.; Fleming, W. W.; Hofer, D. C. *Macromolecules* **1992**, *25*, 582−588.
(19) Lucotte, G.; Cormier, L.; Delfort, B. *J. Polym. Sci., Part A* **1991**, *29*, 897−903.
(20) Sefcik, M. D.; Stejskal, E. O.; McKay, R. A.; Schaefer, J. *Macromolecules* **1979**, *12*, 423−425.
(21) Neenan, T. X.; Whitesides, G. M. *J. Org. Chem.* **1988**, *53*, 2489−2496.
(22) Hale, A.; Macosko, C. W.; Bair, H. E. *Macromolecules* **1991**, *24*, 2610−2621.
(23) Pascault, J. P.; Williams, R. J. J. *J. Polym. Sci., Part B* **1990**, *28*, 25.
(24) Couchman, P. R. *Macromolecules* **1987**, *20*, 1712−1717.
(25) DiBenedetto, A. T. *J. Polym. Sci., Part B* **1987**, *25*, 1949−1969.
(26) Details concerning the MOPAC calculations will be addressed in a forthcoming publication.

MA010339L